Progress In Electromagnetics Research Letters, Vol. 88, 67–74, 2020

Polarization Difference Smoothing in Bistatic MIMO Radar

Karthick Subramaniam[*, 1], Palanisamy Ponnusamy[1], and Srinivasarao Chintagunta[2]

Abstract—This paper investigates the joint direction of departure (DOD) and direction of arrival (DOA) estimation of coherent targets in bistatic multiple-input multiple-output (MIMO) radar under the presence of spatially correlated noise. Based on electromagnetic vector sensors at both transmitter and receiver of MIMO radar, a preprocessing method, namely polarization difference smoothing, is proposed to remove the coherence between targets and to suppress the spatially correlated noise. Then DODs and DOAs are estimated using the ESPRIT method. Further, this paper develops a simple approach for pair-matching between the estimated DODs and DOAs. Simulation results are compared with the receive polarization smoothing and transmit-receive polarization smoothing methods available in literature. Results show that the proposed approach improves the performance significantly.

1. INTRODUCTION

In bistatic MIMO radar, transmitter and receiver arrays are at different locations such that the direction of departure (DOD) and direction of arrival (DOA) are different towards the targets located at far field [1]. For estimating the DOD and DOA of uncorrelated targets, many investigations have been found in literature, for example, estimation of signal parameters via rotational invariance technique (ESPRIT) [2], ESPRIT without pairing [3], multiple signal classification (MUSIC) algorithm [4], trilinear decomposition-based blind algorithm [5], maximum-likelihood algorithm [6], and the references therein. Majority of these investigations were based on high-resolution subspace-based methods such as ESPRIT and MUSIC. In practical applications, the targets are coherent, which leads to a reduction in rank of the signal covariance matrix, and this matrix rank should be restored before employing ESPRIT and MUSIC techniques. Spatial smoothing [7, 8] is a standard approach for decorrelating coherent targets by constructing multiple subarrays and can resolve any number of targets. However, the spatial smoothing technique requires a large number of subarrays proportionately to the number of targets needed to decorrelate. Thus, effective array aperture length becomes smaller as the subarray number increases, and this characteristic leads to the inferiority in performance as well as the number of targets identifiable. In order to overcome this inferiority, electromagnetic vector sensors (EVSs) [9] are employed as sensing elements in passive radar.

The BCD tensor modeling for estimating the joint angle of arrival and polarization in an L-shaped EVSs array is investigated [10]. In [11], a CRB-based transmitting polarization design algorithm is proposed for estimating the 2D angles in a MIMO-EVSs array. Spatial smoothing algorithm in [12, 13] and unitary ESPRIT with inherent smoothing in [14] are used to localize the coherent targets in MIMO radar with EVSs. In [15–17], a polarization smoothing (PS) preprocessing technique is developed to deal with coherent targets by using EVSs in different structures of radar. In [15], PS technique is discussed for a passive linear array with EVSs. In [16], PS is extended for a MIMO radar with scalar sensors at transmitter and EVSs at receiver, and further [17] presents the PS in a bistatic MIMO radar with EVSs at both transmitter and receiver. Compared with the spatial smoothing technique, PS processing is

Received 16 September 2019, Accepted 19 November 2019, Scheduled 9 December 2019

* Corresponding author: Karthick Subramaniam (408113002@nitt.edu).

[1] National Institute of Technology, Tiruchirappalli, India. [2] International Institute of Information Technology, Bhubaneswar, India.

applied to arbitrary array geometry, and it does not reduce the effective array aperture. In both spatial smoothing and polarization smoothing algorithms, rank of the signal covariance matrix can be restored, but they retain noise covariance matrix. Hence the subspace-based techniques with spatial/polarization smoothing are only applicable to spatially uniform white noise.

In [18], considering a planar array with EVSs, a propagator-based method is developed for 2D-DOA estimation of coherent signals in the presence of spatially correlated noise. In [19], spatial difference smoothing in bistatic MIMO radar is used to localize the coherent signals in unknown correlated noise. In [20–22], a method is proposed for angle estimation of targets in bistatic MIMO radar under the presence of spatially correlated noise. In [23], considering a passive uniform rectangular array, a polarization difference smoothing (PDS) method is proposed for simultaneously handling coherent signals and spatially correlated noise. In this paper, we incorporate the PDS approach into a bistatic MIMO radar with EVSs as sensing elements at both transmitter and receiver. The proposed PDS approach with ESPRIT for angle estimation is given in Section 3, and the simulation results to justify the proposed approach are presented in Section 4.

Notation: Vectors and matrices are denoted with lowercase and uppercase bold characters, respectively. $(.)^T$ denotes the transpose, and $(.)^H$ indicates the conjugate-transpose. Symbol $\otimes$ denotes the Kronecker product. $\mathbf{I}_N$ is an $N \times N$ identity matrix; $\mathbf{0}_{M\times N}$ is an $M \times N$ zero matrix; and $diag\{.\}$ represents the diagonal matrix.

2. SIGNAL MODEL

Bistatic MIMO radar is considered with M transmitting and N receiving EVSs (six-component EVSs). The EVSs are positioned uniformly along the z-axis and separated by a distance d_{t} at the transmitter and d_{r} at the receiver. K far-field targets are present in the same range cell. Then, manifold vectors of the transmit array $\mathbf{a}_{\mathrm{t}_k} \in \mathbb{C}^{6M\times 1}$ and receive array $\mathbf{a}_{\mathrm{r}_k} \in \mathbb{C}^{6N\times 1}$ towards the kth target direction are expressed by

$$\begin{aligned} \mathbf{a}_{\mathrm{t}_k} &= \mathbf{b}_{\mathrm{t}_k}(\theta_{\mathrm{t}_k}) \otimes \mathbf{c}_{\mathrm{t}_k}(\theta_{\mathrm{t}_k}, \phi_{\mathrm{t}_k}, \gamma_{\mathrm{t}_k}, \eta_{\mathrm{t}_k}) \\ \mathbf{a}_{\mathrm{r}_k} &= \mathbf{b}_{\mathrm{r}_k}(\theta_{\mathrm{r}_k}) \otimes \mathbf{c}_{\mathrm{r}_k}(\theta_{\mathrm{r}_k}, \phi_{\mathrm{r}_k}, \gamma_{\mathrm{r}_k}, \eta_{\mathrm{r}_k}) \end{aligned} \tag{1}$$

where $\mathbf{b}_{\mathrm{t}_k} = [1, \alpha_k, \cdots, \alpha_k^{M-1}]^T$ in which $\alpha_k = e^{-j2\pi d_{\mathrm{t}} \sin\theta_{\mathrm{t}_k}/\lambda}$ with λ being the wavelength, $\mathbf{b}_{\mathrm{r}_k} = [1, \beta_k, \cdots, \beta_k^{N-1}]^T$ in which $\beta_k = e^{-j2\pi d_{\mathrm{r}} \sin\theta_{\mathrm{r}_k}/\lambda}$, and $\mathbf{c}_{\mathrm{t}_k}/\ \mathbf{c}_{\mathrm{r}_k}$ is the spatial response of the transmitting/ receiving EVS. The spatial response $\mathbf{c}_i, i = \mathrm{t}_k, \mathrm{r}_k$, in vector notation is expressed by

$$\mathbf{c}_i = \begin{bmatrix} c_{1,i} \\ c_{2,i} \\ c_{3,i} \\ c_{4,i} \\ c_{5,i} \\ c_{6,i} \end{bmatrix} = \begin{bmatrix} e_{x,i} \\ e_{y,i} \\ e_{z,i} \\ h_{x,i} \\ h_{y,i} \\ h_{z,i} \end{bmatrix} = \begin{bmatrix} \cos\theta_i \cos\phi_i \sin\gamma_i e^{j\eta_i} - \sin\phi_i \cos\gamma_i \\ \cos\theta_i \sin\phi_i \sin\gamma_i e^{j\eta_i} + \cos\phi_i \cos\gamma_i \\ -\sin\theta_i \sin\gamma_i e^{j\eta_i} \\ -\sin\phi_i \sin\gamma_i e^{j\eta_i} - \cos\theta_i \cos\phi_i \cos\gamma_i \\ \cos\phi_i \sin\gamma_i e^{j\eta_i} - \cos\theta_i \sin\phi_i \cos\gamma_i \\ \sin\theta_i \cos\gamma_i \end{bmatrix} \tag{2}$$

where $0 \le \theta_i < \pi$ is the elevation angle, $0 \le \phi_i < 2\pi$ the azimuth angle, $0 \le \gamma_i < \pi/2$ the auxiliary polarization angle, and $-\pi \le \eta_i < \pi$ the polarization phase difference. Note that these angles are concerned with $i = \mathrm{t}_k, \mathrm{r}_k$.

Let $\mathbf{s}_{m,p}$ be the $P \times 1$ transmitting coded vector signal by the pth element of the mth EVS, which satisfies the orthogonality condition,

$$\mathbf{s}_{m,p}^H \mathbf{s}_{n,q} = \begin{cases} P, & m = n \ \&\ p = q \\ 0, & \text{otherwise} \end{cases};\ m, n = 1, \cdots, M;\ p, q = 1, \cdots, 6.$$

Thus, the total transmission signal by all six elements of all M EVSs is expressed by $6M \times P$ matrix $\mathbf{S} = [\mathbf{S}_1^T, \cdots, \mathbf{S}_M^T]^T$, in which $\mathbf{S}_m = [\mathbf{s}_{m,1}, \cdots, \mathbf{s}_{m,6}]^T$. The transmitted signals steer to K far-field targets are $\{\mathbf{a}_{\mathrm{t}_1}^T \mathbf{S}, \cdots, \mathbf{a}_{\mathrm{t}_K}^T \mathbf{S}\}$. Considering that $\{\zeta_1, \cdots, \zeta_K\}$ are the reflection coefficients of targets,

echoes can be represented by $\{\zeta_1 \mathbf{a}_{\mathrm{t}_1}^T \mathbf{S}, \cdots, \zeta_K \mathbf{a}_{\mathrm{t}_K}^T \mathbf{S}\}$. These echoes are impinging on the receive EVSs. Then, the received signal $\mathbf{X}(l) \in \mathbb{C}^{6N \times P}$ at the lth snapshot is given by

$$\mathbf{X}(l) = \sum_{k=1}^{K} \mathbf{a}_{\mathrm{r}_k} \zeta_k(l) \mathbf{a}_{\mathrm{t}_k}^T \mathbf{S} + \mathbf{V}(l) \tag{3}$$

where $\mathbf{V}(l) \in \mathbb{C}^{6N \times P}$ is the noise matrix at lth snapshot. The signal matrix $\mathbf{X}(l)$ in compact form is given by

$$\mathbf{X}(l) = \mathbf{A}_{\mathrm{r}} \mathbf{\Lambda}(l) \mathbf{A}_{\mathrm{t}}^T \mathbf{S} + \mathbf{V}(l) \tag{4}$$

where $\mathbf{A}_{\mathrm{t}} = [\mathbf{a}_{\mathrm{t}_1}, \cdots, \mathbf{a}_{\mathrm{t}_K}] \in \mathbb{C}^{6M \times K}$ is the manifold matrix of transmit array; $\mathbf{A}_{\mathrm{r}} = [\mathbf{a}_{\mathrm{r}_1}, \cdots, \mathbf{a}_{\mathrm{r}_K}] \in \mathbb{C}^{6N \times K}$ is manifold matrix of receive array; and $\mathbf{\Lambda}(l) = \mathrm{diag}\{\zeta_1(l), \cdots, \zeta_K(l)\} \in \mathbb{C}^{K \times K}$ is the diagonal matrix containing reflection coefficients.

3. PROPOSED APPROACH

3.1. Polarization Difference Smoothing

In polarization difference smoothing, the $6N \times K$ receive array manifold $\mathbf{A}_{\mathrm{r}}$ is divided into six $N \times K$ subarray manifolds $\mathbf{A}_{\mathrm{r},i}$ $(i = 1, \cdots, 6)$, where the ith subarray manifold $\mathbf{A}_{\mathrm{r},i}$ is corresponds to the ith component of all receive EVSs. Thus, the subarray block $\mathbf{A}_{\mathrm{r},1}$ corresponds to $\mathbf{E}_{x,\mathrm{r}} = [\mathbf{e}_{x,\mathrm{r}_1}, \cdots, \mathbf{e}_{x,\mathrm{r}_K}]$, $\mathbf{A}_{\mathrm{r},2}$ corresponds to $\mathbf{E}_{y,\mathrm{r}} = [\mathbf{e}_{y,\mathrm{r}_1}, \cdots, \mathbf{e}_{y,\mathrm{r}_K}]$, $\mathbf{A}_{\mathrm{r},3}$ corresponds to $\mathbf{E}_{z,\mathrm{r}} = [\mathbf{e}_{z,\mathrm{r}_1}, \cdots, \mathbf{e}_{z,\mathrm{r}_K}]$, $\mathbf{A}_{\mathrm{r},4}$ corresponds to $\mathbf{H}_{x,\mathrm{r}} = [\mathbf{h}_{x,\mathrm{r}_1}, \cdots, \mathbf{h}_{x,\mathrm{r}_K}]$, $\mathbf{A}_{\mathrm{r},5}$ corresponds to $\mathbf{H}_{y,\mathrm{r}} = [\mathbf{h}_{y,\mathrm{r}_1}, \cdots, \mathbf{h}_{y,\mathrm{r}_K}]$, and $\mathbf{A}_{\mathrm{r},6}$ corresponds to $\mathbf{H}_{z,\mathrm{r}} = [\mathbf{h}_{z,\mathrm{r}_1}, \cdots, \mathbf{h}_{z,\mathrm{r}_K}]$. The subarray manifolds $\mathbf{A}_{\mathrm{r},i}, i = 1, \cdots, 6$, can be obtained from the receive array manifold $\mathbf{A}_{\mathrm{r}}$ as

$$\mathbf{A}_{\mathrm{r},i} = \begin{bmatrix} \mathbf{r}_i \\ \mathbf{r}_{i+6} \\ \vdots \\ \mathbf{r}_{i+6(N-1)} \end{bmatrix}, \ i = 1, \cdots, 6 \tag{5}$$

where $\mathbf{r}_i$ is the ith row of $\mathbf{A}_{\mathrm{r}}$. The subarray block $\mathbf{A}_{\mathrm{r},i}$ can also be expressed as

$$\mathbf{A}_{\mathrm{r},i} = [\mathbf{b}_{\mathrm{r}_1}(\theta_{\mathrm{r}_1}) c_{i,\mathrm{r}_1}, \cdots, \mathbf{b}_{\mathrm{r}_K}(\theta_{\mathrm{r}_K}) c_{i,\mathrm{r}_K}] = \mathbf{B}_{\mathrm{r}} \mathbf{C}_{i,\mathrm{r}}, \ i = 1, \cdots, 6 \tag{6}$$

where $\mathbf{B}_{\mathrm{r}} = [\mathbf{b}_{\mathrm{r}_1}(\theta_{\mathrm{r}_1}), \cdots, \mathbf{b}_{\mathrm{r}_K}(\theta_{\mathrm{r}_K})]$ and $\mathbf{C}_{i,\mathrm{r}} = \mathrm{diag}\{c_{i,\mathrm{r}_1}, \cdots, c_{i,\mathrm{r}_K}\}$.

Then the received signal $\mathbf{X}_i(l) \in \mathbb{C}^{N \times P}$ corresponds to ith component of the receive EVSs at the lth snapshot which can be expressed from Eq. (3) as

$$\mathbf{X}_i(l) = \mathbf{A}_{\mathrm{r},i} \mathbf{\Lambda}(l) \mathbf{A}_{\mathrm{t}}^T \mathbf{S} + \mathbf{V}_i(l), \ i = 1, \cdots, 6 \tag{7}$$

where $\mathbf{V}_i(l)$ denotes the noise at the ith component of the receive EVSs. The signal $\mathbf{X}_i(l)$, after matched filtering with $\mathbf{S}^H/\sqrt{P}$, is given by

$$\mathbf{X}_{\mathrm{out}_i}(l) = \sqrt{P} \mathbf{A}_{\mathrm{r},i} \mathbf{\Lambda}(l) \mathbf{A}_{\mathrm{t}}^T + \frac{1}{\sqrt{P}} \mathbf{V}_i(l) \mathbf{S}^H \in \mathbb{C}^{N \times 6M}, \ i = 1, \cdots, 6 \tag{8}$$

In order to include inherent smoothing associated with the components of transmitting EVSs, we rearrange the above signal $\mathbf{X}_{\mathrm{out}_i}(l)$ as given below

$$\begin{aligned} \mathbf{Y}_i(l) \ &= \ [\mathbf{x}_{\mathrm{out}_i}^{1,1}(l), \cdots, \mathbf{x}_{\mathrm{out}_i}^{1,N}(l), \mathbf{x}_{\mathrm{out}_i}^{2,1}(l), \cdots, \mathbf{x}_{\mathrm{out}_i}^{2,N}(l), \cdots, \mathbf{x}_{\mathrm{out}_i}^{M,1}(l), \cdots, \mathbf{x}_{\mathrm{out}_i}^{M,N}(l)]^T \in \mathbb{C}^{MN \times 6}, \\ & \quad i = 1, \cdots, 6 \end{aligned} \tag{9}$$

where $\mathbf{x}_{\mathrm{out}_i}^{m,n}(l) \in \mathbb{C}^{6 \times 1}$ represents the signal associated with the ith component of the nth EVS of the receive array corresponding to the mth EVS of the transmit array. The (m,n)th partition $\mathbf{x}_{\mathrm{out}_i}^{m,n}$ at each snapshot can be obtained from the signal $\mathbf{X}_{\mathrm{out}_i}$ in Eq. (8) as $\mathbf{x}_{\mathrm{out}_i}^{m,n} = [\mathbf{X}_{\mathrm{out}_i}(n, 6m-5 : 6m)]^T$. The rearranged signal $\mathbf{Y}_i(l)$ can be expressed in a compact form as

$$\mathbf{Y}_i(l) = \mathbf{B} \mathbf{\Lambda}_{\mathrm{out}}(l) \mathbf{C}_i^T + \mathbf{W}_i(l) = \mathbf{B} \mathbf{D}_i(l) + \mathbf{W}_i(l), \ i = 1, \cdots, 6 \tag{10}$$

where $\mathbf{B} = [\mathbf{b}_{\mathrm{t}_1} \otimes \mathbf{b}_{\mathrm{r}_1}, \cdots, \mathbf{b}_{\mathrm{t}_K} \otimes \mathbf{b}_{\mathrm{r}_K}] \in \mathbb{C}^{MN \times K}, \mathbf{C}_i \triangleq \mathbf{C}_{\mathrm{t}}\mathbf{C}_{i,\mathrm{r}} \in \mathbb{C}^{6 \times K}$ in which $\mathbf{C}_{\mathrm{t}} = [\mathbf{c}_{\mathrm{t}_1}, \cdots, \mathbf{c}_{\mathrm{t}_k}]$ and $\mathbf{C}_{i,\mathrm{r}} = \mathrm{diag}\{c_{i,\mathrm{r}_1}, \cdots, c_{i,\mathrm{r}_K}\}, \mathbf{D}_i(l) = \mathbf{\Lambda}_{\mathrm{out}}(l)\mathbf{C}_i^T, \mathbf{\Lambda}_{\mathrm{out}}(l) = \mathrm{diag}\{\sqrt{P}\zeta_1(l), \cdots, \sqrt{P}\zeta_K(l)\}$, and $\mathbf{W}_i(l)$ is the corresponding noise matrix.

Therefore, the covariance matrix of the signal $\mathbf{Y}_i(l)$ corresponding to the ith component of the receive EVSs can be expressed as

$$\mathbf{R}_{\mathrm{Y},i} = \mathbb{E}\left[\mathbf{Y}_i(l)\mathbf{Y}_i^H(l)\right] \in \mathbb{C}^{MN \times MN},\ i = 1, \cdots, 6 \tag{11}$$

In order to include the smoothing concerning with the components of receive EVSs and to suppress the spatially correlated noise, polarization difference smoothing covariance matrix $\mathbf{R}_{\mathrm{Y}}^{\mathrm{pds}}$ is defined as

$$\mathbf{R}_{\mathrm{Y}}^{\mathrm{pds}} = \sum_{p=1}^{3}\left[\mathbf{R}_{\mathrm{Y},i_p} - \mathbf{R}_{\mathrm{Y},j_p}\right] \tag{12}$$

where indices (i_1, i_2, i_3) are the combination of three different digits formed out of the six digits 1, 2, 3, 4, 5, 6, and indices (j_1, j_2, j_3) are the combination of the remaining three digits. Under the assumption that noise at each component of a receive EVS must be same, difference of covariance matrices $\mathbf{R}_{\mathrm{Y},i}$ will suppress the spatially correlated noise, and their sum will remove the coherence between targets and can resolve up to 36 coherent targets. However, the resolvable target number can be increased two times by incorporating the forward-backward averaging to the polarization difference smoothing matrix $\mathbf{R}_{\mathrm{Y}}^{\mathrm{pds}}$.

3.2. Joint DOD and DOA Estimation Using ESPRIT

The manifold vectors $\mathbf{b}_{\mathrm{t}_k}$ and $\mathbf{b}_{\mathrm{r}_k}$ in matrix $\mathbf{B}$ of Eq. (10) satisfy the rotational invariance property, that is $\mathbf{b}_{\mathrm{t}2_k} = \alpha_k\mathbf{b}_{\mathrm{t}1_k}$ and $\mathbf{b}_{\mathrm{r}2_k} = \beta_k\mathbf{b}_{\mathrm{r}1_k}$, where $\mathbf{b}_{\mathrm{t}1_k}$ ($\mathbf{b}_{\mathrm{r}1_k}$) and $\mathbf{b}_{\mathrm{t}2_k}$ ($\mathbf{b}_{\mathrm{r}2_k}$) denote the first $M-1$ ($N-1$) and last $M-1$ ($N-1$) elements of $\mathbf{b}_{\mathrm{t}_k}$ ($\mathbf{b}_{\mathrm{r}_k}$), respectively. Thus, DOD and DOA can be obtained using ESPRIT. The algorithmic steps for estimating the joint DODs and DOAs are summarized below.

(i) Compute the snapshot covariance matrix of $\mathbf{Y}_i(l)$ using L snapshots as $\hat{\mathbf{R}}_{\mathrm{Y},i} = \frac{1}{6L}\sum_{l=1}^{L}\mathbf{Y}_i(l)\mathbf{Y}_i^H(l)$, where factor 6 is used due to the inherent smoothing.

(ii) Compute the polarization difference smoothing covariance matrix $\mathbf{R}_{\mathrm{Y}}^{\mathrm{pds}}$ using Eq. (12).

(iii) Perform the eigendecomposition of $\mathbf{R}_{\mathrm{Y}}^{\mathrm{pds}}$ to construct the signal-subspace $\mathbf{E}_{\mathrm{s}} \in \mathbb{C}^{MN \times K}$ and noise-subspace $\mathbf{E}_{\mathrm{n}} \in \mathbb{C}^{MN \times (MN-K)}$, where columns of $\mathbf{E}_{\mathrm{s}}$ and $\mathbf{E}_{\mathrm{n}}$ are the eigenvectors corresponding to K largest eigenvalues and the remaining $MN-K$ eigenvalues of $\mathbf{R}_{\mathrm{Y}}^{\mathrm{pds}}$, respectively.

(iv) For DOD estimation, compute eigenvalues $\{\lambda_{\mathrm{t}_1}, \lambda_{\mathrm{t}_2}, \cdots, \lambda_{\mathrm{t}_K}\}$ of $\mathbf{\Psi}_{\mathrm{t}} = (\mathbf{E}_{\mathrm{t}1}^H\mathbf{E}_{\mathrm{t}1})^{-1}\mathbf{E}_{\mathrm{t}1}^H\mathbf{E}_{\mathrm{t}2}$, where $\mathbf{E}_{\mathrm{t}1} = \mathbf{J}_1\mathbf{E}_{\mathrm{s}}$ and $\mathbf{E}_{\mathrm{t}2} = \mathbf{J}_2\mathbf{E}_{\mathrm{s}}$ in which $\mathbf{J}_1 = \left[\mathbf{I}_{(M-1)N} \mid \mathbf{0}_{(M-1)N \times N}\right]$ and $\mathbf{J}_2 = \left[\mathbf{0}_{(M-1)N \times N} \mid \mathbf{I}_{(M-1)N}\right]$. Then, the DOD estimates are

$$\hat{\theta}_{\mathrm{t}_k} = \sin^{-1}\left(\frac{\arg(\lambda_{\mathrm{t}_k})}{-2\pi d_{\mathrm{t}}/\lambda}\right), \quad k = 1, \cdots, K. \tag{13}$$

(v) For DOA estimation, compute eigenvalues $\{\lambda_{\mathrm{r}_1}, \lambda_{\mathrm{r}_2}, \cdots, \lambda_{\mathrm{r}_K}\}$ of $\mathbf{\Psi}_{\mathrm{r}} = (\mathbf{E}_{\mathrm{r}1}^H\mathbf{E}_{\mathrm{r}1})^{-1}\mathbf{E}_{\mathrm{r}1}^H\mathbf{E}_{\mathrm{r}2}$, where $\mathbf{E}_{\mathrm{r}1} = \mathbf{J}_3\mathbf{E}_{\mathrm{s}}$ and $\mathbf{E}_{\mathrm{r}2} = \mathbf{J}_4\mathbf{E}_{\mathrm{s}}$ in which $\mathbf{J}_3 = \mathbf{I}_M \otimes \left[\mathbf{I}_{(N-1)} \mid \mathbf{0}_{(N-1)\times 1}\right]$ and $\mathbf{J}_4 = \mathbf{I}_M \otimes \left[\mathbf{0}_{(N-1)\times 1} \mid \mathbf{I}_{(N-1)}\right]$. Then, the DOA estimates are

$$\hat{\theta}_{\mathrm{r}_k} = \sin^{-1}\left(\frac{\arg(\lambda_{\mathrm{r}_k})}{-2\pi d_{\mathrm{r}}/\lambda}\right), \quad k = 1, \cdots, K. \tag{14}$$

(vi) For pairing the DODs and DOAs, we utilize the principle that columns of $\mathbf{B}$ are orthogonal to columns of $\mathbf{E}_{\mathrm{n}}$. Thus, pairing between $\hat{\theta}_{\mathrm{t}_k}$ and $\hat{\theta}_{\mathrm{r}_k}$ of a particular target can be obtained by finding $f(\hat{\theta}_{\mathrm{t}_k}, \hat{\theta}_{\mathrm{r}_p}) \triangleq \mathbf{b}^H(\hat{\theta}_{\mathrm{t}_k}, \hat{\theta}_{\mathrm{r}_p})\mathbf{E}_{\mathrm{n}}\mathbf{E}_{\mathrm{n}}^H\mathbf{b}(\hat{\theta}_{\mathrm{t}_k}, \hat{\theta}_{\mathrm{r}_p}),\ k, p = 1, \cdots, K$, and selecting the angle indexed by the minimum value concerning $\hat{\theta}_{\mathrm{r}_p}$ for each $\hat{\theta}_{\mathrm{t}_k}$, where $\mathbf{b}(\hat{\theta}_{\mathrm{t}_k}, \hat{\theta}_{\mathrm{r}_p}) = \mathbf{b}_{\mathrm{t}_k}(\hat{\theta}_{\mathrm{t}_k}) \otimes \mathbf{b}_{\mathrm{r}_k}(\hat{\theta}_{\mathrm{r}_k})$.

4. SIMULATION RESULTS

Monte-Carlo simulations are presented here to evaluate the accuracy and precision performance of the proposed polarization difference smoothing (TrRr-PDS) under the presence of coherent targets and spatially correlated noise. The performance is compared with the existing receiver polarization smoothing (Rr-PS) [16] and transmitter-receiver polarisation smoothing (TrRr-PS) [17]. Accuracy is described by the averaged root mean squared error (RMSE) of direction estimates, defined by

$$\text{RMSE} \triangleq \sqrt{\frac{1}{2KM_c}\sum_{i=1}^{M_c}\sum_{k=1}^{K}\left[\left(\hat{\theta}_{\text{t}_{k,i}}-\theta_{\text{t}_k}\right)^2+\left(\hat{\theta}_{\text{r}_{k,i}}-\theta_{\text{r}_k}\right)^2\right]} \tag{15}$$

where $\hat{\theta}_{\text{t}_{k,i}}/\hat{\theta}_{\text{r}_{k,i}}$ is the estimate of $\theta_{\text{t}_k}/\theta_{\text{r}_k}$ at ith Monte-Carlo trial, and M_c is the total number of executed trials.

In all simulations, we consider $M = N = 10$ EVSs with spacing $d_{\text{t}} = d_{\text{r}} = \lambda/2$ at both transmitter and receiver, Hadamard matrix of order $P = 64$ for generation of the transmission signal $\mathbf{S}$, $L = 100$ snapshots (except for Fig. 2 in which L varies from 10 to 200), and $M_c = 500$ Monte-Carlo trials are executed. The spatially correlated noise is generated such that its covariance matrix $\mathbf{R}_v$ is given by

$$\mathbf{R}_{v[k,l]} = \begin{cases}\sigma^2, & k=l\\ \sigma^2\rho^{|k-l|}e^{j\pi(k-l)/N}, & otherwise\end{cases};\ k,l=\{1,\cdots,N\}; \tag{16}$$

where $\rho^{|k-l|}$ is the correlation coefficient between the kth and lth EVSs, and σ^2 is the noise power. The noise power σ^2 is chosen in accordance with the provided signal to noise ratio (SNR) and signal power $\sigma_\zeta^2 \triangleq \frac{1}{K}\sum_{k=1}^{K}\mathbb{E}[\zeta_k(l)\zeta_k^H(l)]$. Note that $\rho = 0$ for spatially white noise.

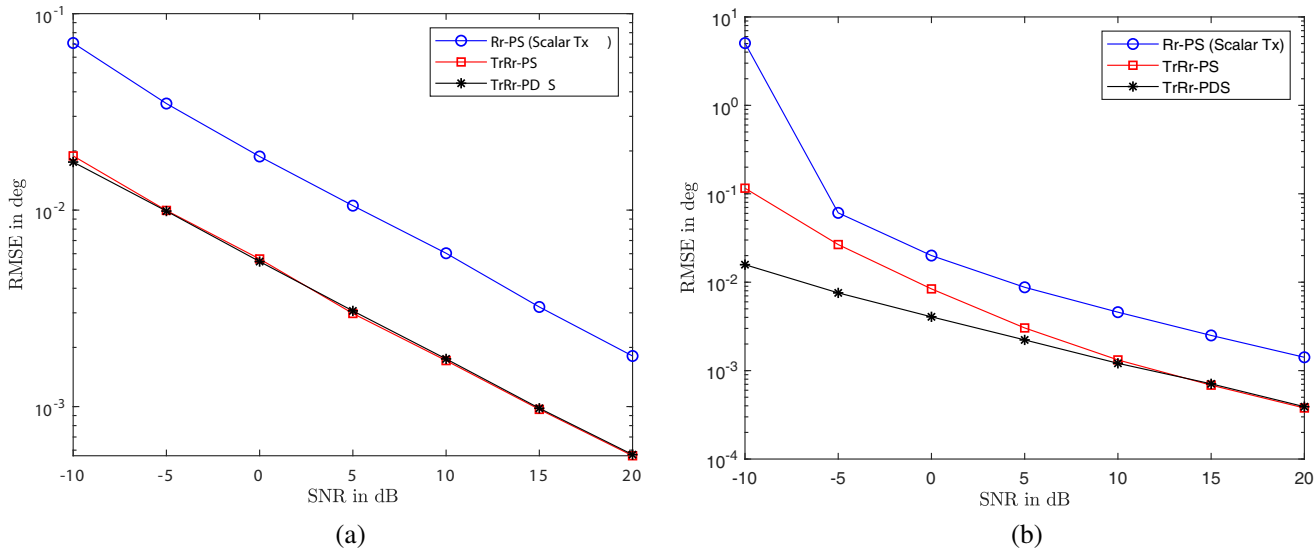

Figure 1. RMSE versus SNR. (a) Spatially white noise. (b) Spatially correlated noise.

Figures 1, 2, and 3 illustrate the RMSE of direction estimates versus SNR, snapshot number L, and correlation coefficient ρ, respectively. In these evaluations, we set $K = 3$ coherent targets with $\theta_{\text{t}} = \{10^\circ, 16^\circ, 23^\circ\}$, $\theta_{\text{r}} = \{26^\circ, 13^\circ, 20^\circ\}$, $\phi_{\text{t}} = \{120^\circ, 30^\circ, 40^\circ\}$, $\phi_{\text{r}} = \{25^\circ, 35^\circ, 145^\circ\}$, $\gamma_{\text{t}} = \{15^\circ, 20^\circ, 45^\circ\}$, $\gamma_{\text{r}} = \{45^\circ, 30^\circ, 60^\circ\}$, $\eta_{\text{t}} = \{1.5708, -0.7854, 0.7854\}$, and $\eta_{\text{r}} = \{-1.5708, 1.0472, 0.5236\}$. Reflection coefficients of coherent targets are generated by $\zeta_k(l) = \epsilon_k\zeta_0(l)$, where $(\epsilon_1, \epsilon_2, \epsilon_3) = (1, 1+1.2j, 1-j)$ and $\{\zeta_0(1), \cdots, \zeta_0(L)\}$ are the complex normalized Gaussian samples. SNR ranges from -10 dB to 20 dB with interval of 5 dB in Fig. 1, and constant at 0 dB in both Fig. 2 and Fig. 3. In Fig. 1 and Fig. 2, correlation factor ρ of correlated noise is taken as 0.98 whereas in Fig. 3 ρ varies from 0 to 1 with 0.1 step size. Fig. 1(a) evaluates RMSE versus SNR under the presence of spatially white noise, and

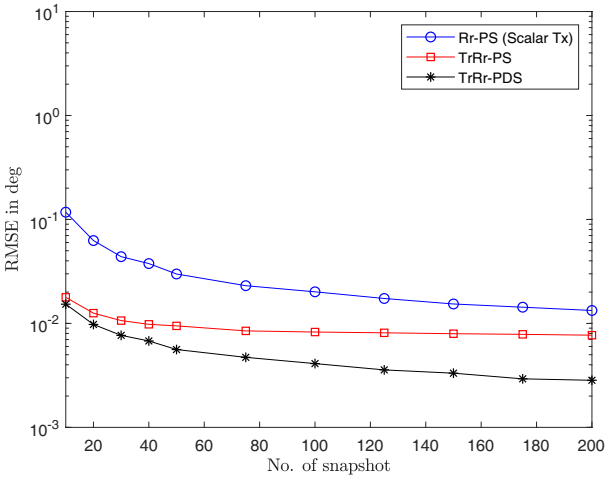

Figure 2. RMSE versus snapshot number under the presence of spatially correlated noise.

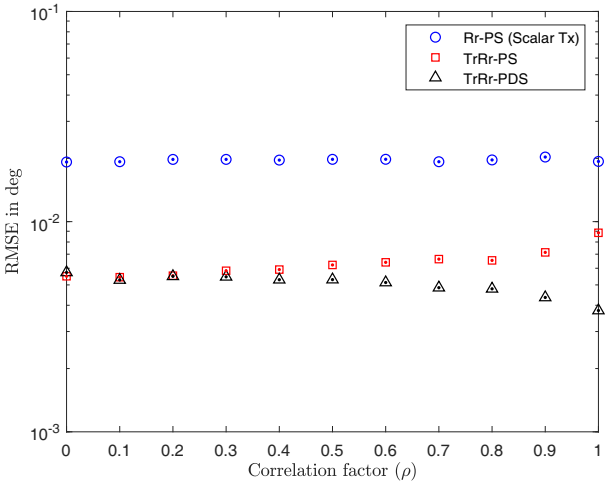

Figure 3. RMSE versus correlation factor ρ of correlated noise.

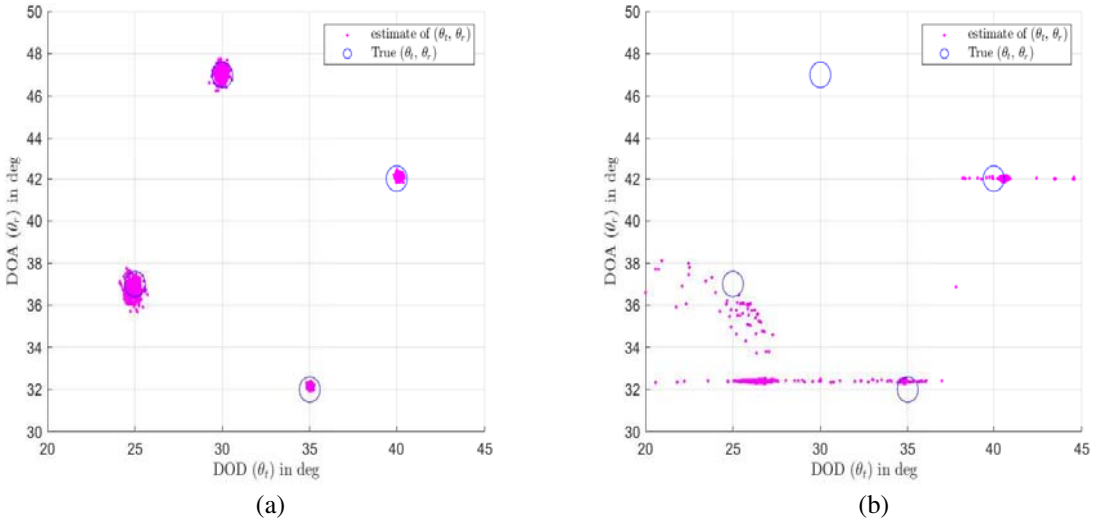

Figure 4. Scatters of $(\hat{\theta}_{\mathrm{t}}, \hat{\theta}_{\mathrm{r}})$ using the method in [16]. (a) Uncorrelated noise. (b) Correlated noise.

Fig. 1(b) evaluates that in spatially correlated noise. The RMSE in Fig. 1, Fig. 2, and Fig. 3 signify that the accuracy performance of the proposed PDS approach is superior significantly at low SNR as compared with the approaches in [16] and [17]. This superior performance is due to the smoothing factor as well as the removal of noise. Note that the smoothing factors of the proposed method and the method in [17] are the same which is 36, whereas the smoothing factor of the method in [16] is 6.

Figures 4, 5, and 6 show both accuracy and precision performances through the scatters of DOD and DOA estimates executed over 500 independent trials. Figs. 4–6 also describe the pairing between DOD and DOA estimates. In this analysis, we consider $SNR = 0\,\mathrm{dB}$, $\rho = 0.85$ for correlated noise, and $K = 4$ coherent targets with $(\epsilon_1, \epsilon_2, \epsilon_3, \epsilon_4) = (1, 1+1.2j, 2-j, 4-j)$, $\theta_{\mathrm{t}} = \{25°, 30°, 35°, 40°\}$, $\theta_{\mathrm{r}} = \{37°, 47°, 32°, 42°\}$, $\phi_{\mathrm{t}} = \{32°, 55°, 46°, 64°\}$, $\phi_{\mathrm{r}} = \{26°, 42°, 35°, 56°\}$, $\gamma_{\mathrm{t}} = \{45°, 45°, 45°, 45°\}$, $\gamma_{\mathrm{r}} = \{31°, 60°, 40°, 70°\}$, $\eta_{\mathrm{t}} = \{-1.5708, 1.0472, 0.7854, 0.5236\}$, and $\eta_{\mathrm{r}} = \{0.7854, 0.5236, -1.0472, 0.6283\}$. With the pairing approach described in step-vi of section 3.2, the estimates of DODs and DOAs are paired accurately. The scatters of DOD and DOA estimated in Fig. 4, Fig. 5, and Fig. 6 show that the accuracy performance of the proposed method (Fig. 6) is significantly relative to the methods in [16] (Fig. 4) and [17] (Fig. 5).

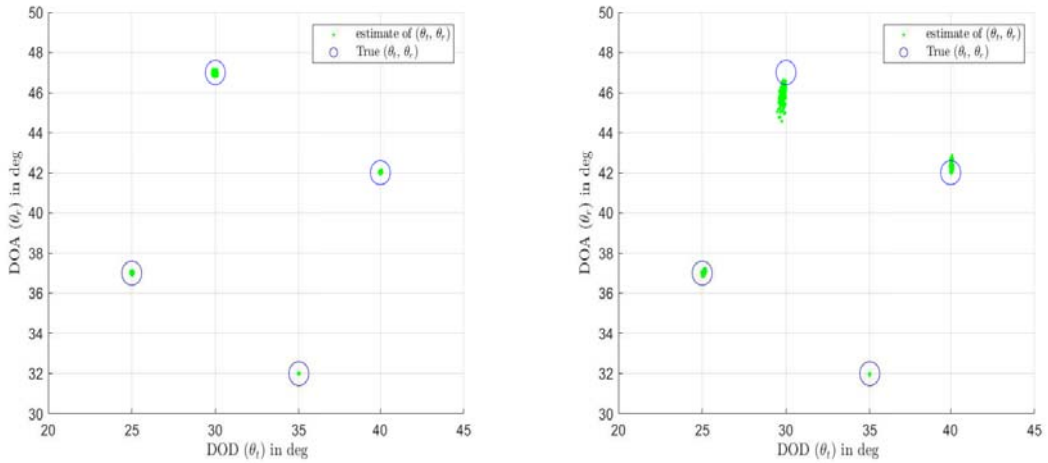

Figure 5. Scatters of $(\hat{\theta}_{\mathrm{t}}, \hat{\theta}_{\mathrm{r}})$ using the method in [17]. (a) Uncorrelated noise. (b) Correlated noise.

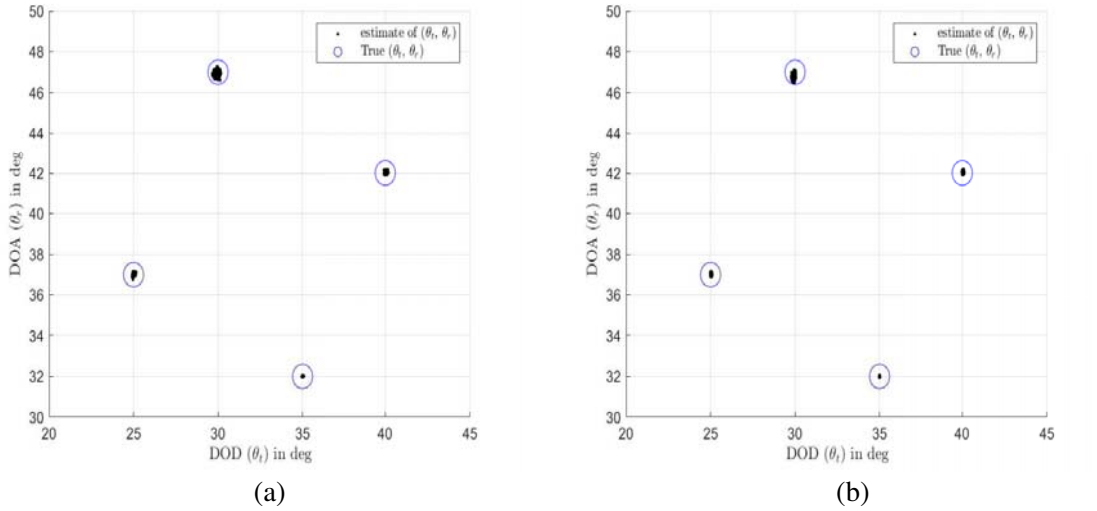

Figure 6. Scatters of $(\hat{\theta}_{\mathrm{t}}, \hat{\theta}_{\mathrm{r}})$ using the proposed method. (a) Uncorrelated noise. (b) Correlated noise.

5. CONCLUSION

A polarization difference smoothing preprocessing approach is proposed for a bistatic MIMO radar to deal with coherent targets and spatially correlated noise. Simulation results show that the proposed approach outperforms the existing polarization smoothing based methods, particularly at low signal to noise ratio region. Further, the DOD and DOA estimates are paired accurately with a simple procedure developed using the orthogonality between noise subspace and manifold vector of estimated angles.

REFERENCES

1. Li, J. and P. Stoica, "MIMO radar with colocated antennas," *IEEE Signal Process. Mag.*, Vol. 24, No. 5, 106–114, 2007.
2. Duofang, C., C. Baixiao and Q. Guodong, "Angle estimation using ESPRIT in MIMO radar," *Electron. Lett.*, Vol. 44, No. 12, 770–771, 2008.

3. Jinli, C., G. Hong, and S. Weimin, "Angle estimation using ESPRIT without pairing in MIMO radar," *Electronics Letters*, Vol. 44, No. 24, 1422–1423, 2008.
4. Li, J., X. Zhang, R. Cao, and M. Zhou, "Reduced-dimension MUSIC for angle and array gain-phase error estimation in bistatic MIMO radar," *IEEE Commun. Lett.*, Vol. 17, No. 3, 443–446, 2013.
5. Zhang, X., X. Gao, G. Feng, and D. Xu, "Blind joint DOA and DOD estimation and identifiability results for MIMO radar with different transmit/receive array manifolds," *Progress In Electromagnetics Research B*, Vol. 18, 101–119, 2009.
6. Chen, H. W., D. Yang, H.-Q. Wang, X. Li, and Z. Zhuang, "Direction finding for bistatic MIMO radar using EM maximum likelihood algorithm," *Progress In Electromagnetics Research*, Vol. 141, 99–116, 2013.
7. Pillai, S. U. and B. H. Kwon, "Forward/backward spatial smoothing techniques for coherent signal identification," *IEEE Trans. Acoust., Speech, Signal Process.*, Vol. 37, No. 1, 8–15, 1989.
8. Ma, X., X. Dong, and Y. Xie, "An improved spatial differencing method for DOA estimation with the coexistence of uncorrelated and coherent signals," *IEEE Sensors J.*, Vol. 16, No. 10, 3719–3723, 2016.
9. Nehorai, A. and E. Paldi, "Vector-sensor array processing for electromagnetic source localization," *IEEE Trans. Signal Process.*, Vol. 42, No. 2, 376–398, 1994.
10. Gao, Y.-F. and Q. Wan, "A rank-$(L, L, 1)$ BCD based AOA-polarization joint estimation algorithm for electromagnetic vector sensor array," *Progress In Electromagnetics Research M*, Vol. 56, 25–32, 2017.
11. Zheng, G. and B.-X. Chen, "Optimal polarization design for direction finding using mimo electromagnetic vector-sensor array," *Progress In Electromagnetics Research C*, Vol. 42, 205–212, 2013.
12. Chintagunta, S. and P. Palanisamy, "DOD and DOA estimation using the spatial smoothing in MIMO radar with the EmV sensors," *Multidim Syst Sign Process*, Vol. 29, No. 4, 1241–1253, 2018.
13. Chintagunta, S. and P. Ponnusamy, "Spatial and polarization angle estimation of mixed-targets in MIMO radar," *Progress In Electromagnetics Research M*, Vol. 82, 49–59, 2019.
14. Ponnusamy, P., K. Subramaniam, and S. Chintagunta, "Computationally efficient method for joint DOD and DOA estimation of coherent targets in MIMO radar," *Signal Processing*, Vol. 165, 262–267, 2019.
15. Rahamim, D., J. Tabrikian, and R. Shavit, "Source localization using vector sensor array in a multipath environment," *IEEE Trans. Signal Process.*, Vol. 52, No. 11, 3096–3103, 2004.
16. Zheng, G. and B. Wu,"Polarisation smoothing for coherent source direction finding with multiple-input and multiple-output electromagnetic vector sensor array," *IET Signal Processing*, Vol. 10, No. 8, 873–879, 20016.
17. Chintagunta, S. and P. Ponnusamy, "Integrated polarisation and diversity smoothing algorithm for DOD and DOA estimation of coherent targets," *IET Signal Processing*, Vol. 12, No. 4, 447–453, 2018.
18. Gu, C., J. He, X. Zhu, and Z. Liu, "Efficient 2D DOA estimation of coherent signals in spatially correlated noise using electromagnetic vector sensors," *Multidim Syst Sign Process*, Vol. 21, No. 3, 239–254, 2010.
19. Hong, S., X. Wan, and H. Ke, "Spatial difference smoothing for coherent sources location in MIMO radar," *Signal Processing*, Vol. 109, 69–83, 2015.
20. Wen, F., X. Xiong, J. Su, and Z. Zhang, "Angle estimation for bistatic MIMO radar in the presence of spatial colored noise," *Signal Processing*, Vol. 134, 261–267, 2017.
21. Jiang, H., J. Zhang, and K. M. Wong, "Joint DOD and DOA estimation for bistatic MIMO radar in unknown correlated noise," *IEEE Trans. Veh. Technol.*, Vol. 64, No. 11, 5113–5125, 2015.
22. Jin, M., G. Liao, and J. Li, "Joint DOD and DOA estimation for bistatic MIMO radar," *Signal Processing*, Vol. 89, No. 2, 244–251, 2009.
23. He, J., S. Jiang, J. Wang, and Z. Liu, "Polarization difference smoothing for direction finding of coherent signals," *IEEE Trans. Aerosp. Electron. Syst.*, Vol. 46, No. 1, 469–480, 2010.